

The Gene Fitness Atlas

A Roadmap for Predicting Evolution

September 2024

Aishwarya Deshpande

Yi-Syuan Guo

Allan Scott

Andrew Frank

Katrina Waters

Jayde Aufrecht

DISCLAIMER

This report was prepared as an account of work sponsored by an agency of the United States Government. Neither the United States Government nor any agency thereof, nor Battelle Memorial Institute, nor any of their employees, makes **any warranty, express or implied, or assumes any legal liability or responsibility for the accuracy, completeness, or usefulness of any information, apparatus, product, or process disclosed, or represents that its use would not infringe privately owned rights.** Reference herein to any specific commercial product, process, or service by trade name, trademark, manufacturer, or otherwise does not necessarily constitute or imply its endorsement, recommendation, or favoring by the United States Government or any agency thereof, or Battelle Memorial Institute. The views and opinions of authors expressed herein do not necessarily state or reflect those of the United States Government or any agency thereof.

PACIFIC NORTHWEST NATIONAL LABORATORY
operated by
BATTELLE
for the
UNITED STATES DEPARTMENT OF ENERGY
under Contract DE-AC05-76RL01830

Printed in the United States of America

Available to DOE and DOE contractors from
the Office of Scientific and Technical Information,
P.O. Box 62, Oak Ridge, TN 37831-0062

www.osti.gov

ph: (865) 576-8401

fox: (865) 576-5728

email: reports@osti.gov

Available to the public from the National Technical Information Service
5301 Shawnee Rd., Alexandria, VA 22312

ph: (800) 553-NTIS (6847)

or (703) 605-6000

email: info@ntis.gov

Online ordering: <http://www.ntis.gov>

The Gene Fitness Atlas

A Roadmap for Predicting Evolution

September 2024

Aishwarya Deshpande
Yi-Syuan Guo
Allan Scott
Andrew Frank
Katrina Waters
Jayde Aufrecht

Prepared for
the U.S. Department of Energy
under Contract DE-AC05-76RL01830

Pacific Northwest National Laboratory
Richland, Washington 99354

Abstract

We developed a novel, high-throughput microfluidic device design containing “interaction zones” where progeny cell lines compete against each other allowing for accurate analysis of bacterial cell fitness. The goal of the project was to use the device for two applications: 1) gene knockout screening and 2) antibiotic resistance screening. The microfluidic platform was fabricated using photolithography and soft lithography in polydimethylsiloxane (PDMS). *E.coli* Keio mutants and fluorescent wildtype parent were chosen for the study. Cells were grown overnight and their loading into the devices and seeding in mother machines was optimized. For mutant screening, the least fit mutant and wildtype parent were cultured individually and then added to the microfluidic device. The mother machines which were seeded with mutant and wildtype were imaged through time lapse microscopy and the growth of cells was observed. For antibiotic screening, wildtype *E.coli* cells which were grown overnight were added to the device and washed with media containing the antibiotic ampicillin. The growth pattern in presence and absence of ampicillin was observed through time lapse microscopy. It was observed that over a period of four hours, both the mutant and the wildtype divided in the mother machine and pushed daughter cells out into the interaction zone. In case of the antibiotic screening experiment, the fluorescent wildtype divided both in the absence and presence of sublethal concentration of ampicillin. This study is a proof of concept demonstration of high- throughput single cell analysis of cells using a novel microfluidics device.

Acknowledgments

This research was supported by the Open Call Investment under the Laboratory Directed Research and Development (LDRD) Program at Pacific Northwest National Laboratory (PNNL). PNNL is a multi-program national laboratory operated for the U.S. Department of Energy (DOE) by Battelle Memorial Institute under Contract No. DE-AC05-76RL01830.

Acronyms and Abbreviations

PDMS	Poly di-methylsiloxane
WT	Wildtype
RFP	Red fluorescent protein
OD	Optical Density
LB	Luria Bertani media
PBS	phosphate buffer saline
BSA	bovine serum albumin
F	fluorescent
NF	non-fluorescent

Contents

Abstract.....	ii
Acknowledgments.....	iii
Acronyms and Abbreviations.....	iv
1.0 Introduction	1
2.0 Materials and Methods	3
2.1 Chip Design and Fabrication	3
2.2 <i>E.coli</i> Mutant Library and Fluorescence	3
2.3 Bulk Experiments.....	3
2.4 Chip Loading and Optimization	4
2.5 Particle image velocimetry in interaction zone.....	4
2.6 Time Series Experiment with Antibiotics	5
2.7 Time series experiment with less fit mutant and wild type	5
3.0 Results and Discussion	6
3.1 Mutant Screening Platform Design and Fabrication	6
3.2 Bulk Competition Experiments	6
3.3 Particle image velocimetry and flow simulations in interaction zones	7
3.4 Mother machine seeding and wash out.....	8
3.5 Cell Replication in Mother Machines	9
3.6 Continued replication and inoculation of interaction zones	9
3.7 Growth in presence on antibiotic Ampicillin	10
3.8 Competition between wildtype and mutant strains.....	10
4.0 References.....	13

Figures

Figure 1: The novel mutant screening design leverages 65 parallel microfluidic reactors that trap individual mother cells and force their progeny to compete in a highly controlled interaction zone.....	1
Figure 2: A) The microfluidic mutant screening platform was designed to have one inlet and 65 outlets for high-throughput experimentation. B) Two mother machines (1 μ m wide) seed each interaction zone (25 or 50 μ m wide). C) the AutoCAD design includes two layers: 1.4 μ m deep mother machines (red), 20 μ m deep other channels (white). D) the PDMS mold shows the replication accuracy of the design.....	6
Figure 3 : Particle image velocimetry of interaction zones. A) Laminar flow simulations (COMSOL) through the interaction zones show theoretical velocities down to 0.01 μ m/s in the when flow to the design inlet was set to 1 μ L/hr. Speeds of fluorescent beads under flow of a) 1 μ L/min, b) 0.5 μ L/min and c) 10 μ L/hr were calculated using particle image velocimetry.....	8

Figure 4: Time series images of <i>E.coli</i> mother cells in mother machines dividing into two daughter cells. Images were taken every 30 minutes on confocal microscope under 63X in bright field and RFP light.....	9
Figure 5 Time series images showing growth of cells in mother machines and pushing daughter cells in the interaction zone.....	10
Figure 6. Time series images taken every 30 minutes of growth of <i>E.coli</i> cells in mother machine in presence of Ampicillin	11
Figure 7. Time series images of growth of less fit mutant and parent wildtype <i>E.coli</i> (red fluorescent) cells in mother machines	12

Tables

Table 1. <i>E.coli</i> mutants chosen and their plate locations from the Keio library	4
Table 1. Percentage of fluorescent cells from mixed cultures as calculated from Novocyte flow cytometer	7

1.0 Introduction

In 1859 when Charles Darwin first observed that natural selection was driven by the “survival of the fittest,” he did not have the knowledge that we have today: most evolution is not directed by gene mutations with strongly advantageous fitness effects. In fact, the majority of evolution is driven either by random processes (i.e. genetic drift) or by gene mutations that only slightly influence the organism’s fitness (i.e. neutral mutations). However, nearly 200 years after Darwin posited his theory of evolution, scientists are still debating how much these neutral mutations can contribute to an organisms’ overall fitness, in part because these small contributions are obscured in experiments by the stochastic noise of genetic drift. If we did have the ability to quantify the fitness contributions of each gene - including neutral genes - and higher order gene interactions, then we could predict how that species could evolve.

Predicting evolution has many beneficial applications for human health. For example, we could predict how a pathogen could evolve resistance to antibiotics, or how individual microbial members evolve to throw off the balance in the host microbiome. To identify and prevent potential infectious disease outbreaks before they begin, there is a critical need for a way to predict the evolution and emergence of novel pathogens. To get the quantity and quality of data required to predict a species’ evolution, however, requires a new experimental approach to mutant screening. The overall goal for this work is to develop a microfluidic based mutant screen that could measure the the “probability of fixation”, for individual gene knockout mutants. The highthroughput nature of the microfluidic screen will enable entire mutant libraries to be screened and the data to be compiled into an open-source repository - the Gene Fitness Atlas.

The mutant screening approach developed in this work is founded on microfluidics technology, chosen for its superb liquid handling and automation capabilities, paired with fluorescence microscopy. The microfluidic platform is composed of 65 microscale reactors

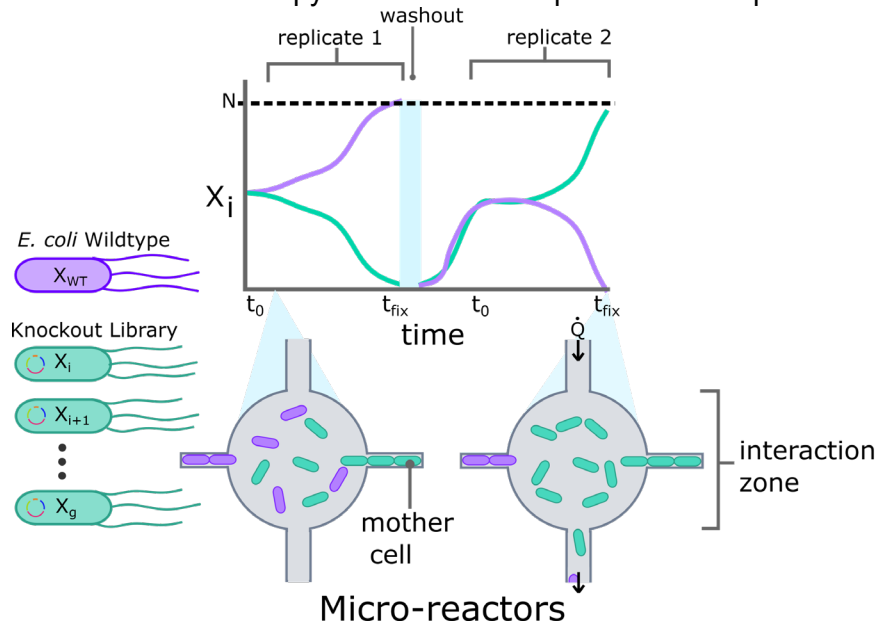


Figure 1: The novel mutant screening design leverages 65 parallel microfluidic reactors that trap individual mother cells and force their progeny to compete in a highly controlled interaction zone.

running in parallel (Figure 1). Within each reactor is an “interaction zone” where a subpopulation of cells will compete after they are generated from two mother cells. The mother cells (i.e. one gene knockout mutant and one RFP-producing wildtype *E. coli* cell) will each be trapped at the dead end of two narrow channels (i.e. mother machines). As the mother cells replicate and push daughter cells into the interaction zone, the progeny mutant line will directly compete for resources with the progeny wildtype line, while the immortalized

mother cells face no evolutionary pressure. To control the size of the subpopulation, we

maintain a constant flow rate, Q , through the interaction zone. This ensures that one of the two strains will “fix”, or become the dominant strain, over time. Once a strain has fixed, we increase Q to wash out the interaction zone and can repeat the experiment several more times with the exact same mother cells. The benefit of this design is that the highly controlled experimental replication will ultimately reduce stochastic noise between replicates and allow researchers to parse the fitness effects of neutral mutations from random genetic drift.

2.0 Materials and Methods

2.1 Chip Design and Fabrication

The microfluidic mutant screening platform was designed in AutoCad to include 1 inlet and 65 interaction zones each with their own outlet (Figure 2). The design includes 2 layers for fabrication: 1. A layer containing only the mother machines and 2. A layer containing all other channels. Using standard photolithography methods and a Bosch etch these two layers were fabricated sequentially on the same silicon wafer so that the mother machines were 1.4 μm deep and all other channels were 20 μm deep. Microfluidic molds were created from the silicon wafer using soft-lithography in poly-dimethylsiloxane (PDMS). Prior to molding, the wafer was treated with silane ((Trichloro(1H,1H,2H,2H-perfluoro-n-octyl)silane), 85°C, 60 min) to prevent adhesion of the PDMS (Whitesides and Stroock 2001).

The microfluidic devices were constructed in lab from the wafer by mixing polydimethylsiloxane (PDMS) with curing agent in 10:1 ratio (Bergmiller et al. 2017; Whitesides and Stroock 2001). After degassing for 15-20 minutes under vacuum, curing was done in an oven at 65°C for 1.5 hours. The PDMS chips were then cut from the molds around the wafer and holes were punched into the inlet and outlets with a 1.5 mm biopsy punch. The PDMS chips and glass coverslips (size 2) were cleaned by dipping in isopropanol and dried at room temperature. The chips were then cleaned with tape and treated with oxygen plasma to bond the chips to coverslips. After bonding, the devices were placed in oven at 65°C for 5 minutes to strengthen the bonding and degassed for 5 minutes to remove any air bubbles before filling.

2.2 *E.coli* Mutant Library and Fluorescence

The Keio *E.coli* mutant library was obtained from GenoBase (Baba et al. 2006). The Keio *E.coli* K12 mutant library consists of 3985 single gene knockout mutants (Baba et al. 2006). The wildtype parent strain was genetically modified to fluoresce by adding the fluorescent marker mKate2 which is a red fluorescent protein (RFP) and kanamycin as the antibiotic marker. This was done to aid in easy visualization and differentiation from mutant *E.coli* cells on the confocal microscope.

2.3 Bulk Experiments

Based on the fitness scores (average taken across all fitness scores), the most fit, least fit and similar fit *E.coli* mutants from the Keio library were chosen (Nichols et al. 2011). These were chosen based on comparison of their average fitness scores with wild type parent. The three mutants (Table 1) and fluorescent wildtype *E.coli* parent strain were cultured individually in Luria Bertani (LB) broth (Fisher Bioreagents) and incubated overnight at 37°C with 100 RPM shaking in a shaker incubator (MaxQ4450, Thermo Scientific). The next day, optical density (OD) was measured at 600 nm for each tube using NanoDrop (Thermo Scientific). Based on OD values, equal amount of culture from each strain was added to create mixed cultures of each mutant with the fluorescent parent. Each mixed culture had 8 replicates. As a control, the fluorescent parent was inoculated again from the previous culture. All tubes were incubated at 37°C with 100 RPM shaking overnight. The next day, fluorescence measurements were taken for all replicates and the parent strain with NovoCyte 2 flow cytometer (Agilent Technologies) in a 96 well plate containing 2 μL culture and 200 μL 1X phosphate buffered saline (PBS).

Table 1. *E.coli* mutants chosen and their plate locations from the Keio library

<i>E.coli</i> Mutant	Fitness	Location in library
ECK0324-YAHL	Equal fit	Plate 5- E9 well
ECK2902-UBIH	Most fit	Plate 79- B10 well
ECK2504-GUAB	Least fit	plate 69- A4 well

2.4 Chip Loading and Optimization

E.coli cells grown overnight were centrifuged at 5000 rpm for 5 minutes and cell pellets were resuspended in supernatant to reduce the volume to 1/10th of the original volume. Bovine serum albumin (BSA, Sigma Aldrich) was added to the concentrated cells and after brief vortexing in pulses (Vortex Genie 2), cells were added to the mutant screening platform with syringe pump (Braintree Scientific, Inc). The mutant screening platform was then incubated at room temperature overnight to allow cells to move into the mother machines. The next day, the mutant screening platforms were observed on scanning confocal microscope (Leica Microsystems DmRXE) while connected to syringe pump. To wash out the cells in channels, a flow of 2 μ L/min was used (details of flow fluid are in the paragraph below). Flow was stopped when ~70% of cells appeared to be washed out. Media was also flown in from each outlet to ensure removal of any blockages and cells. This was followed by incubation of the chip at room temperature for 2-3 hours to allow seeding of mother machines. Once at least 3-4 of the mother machines were seeded fully, time series experiment was started.

Several optimization steps were conducted to ensure that mother machines were seeded with *E.coli* cells. Different speeds of centrifugation were attempted in centrifuge adapter for slides (CombiSlide Adapter, Eppendorf) to ensure that cover slips did not break during the centrifugation. The speed of 100 Xg for 1-2 minutes was selected as the optimum speed. Although the centrifugation did not significantly affect the seeding of mother machines with fluorescent cells, it helped in creating a state of flow in the device. Coverslips of size 1 (0.13-0.17 mm, Ted Pella, Inc.) were initially used for bonding to PDMS devices. However, they were fragile and broke easily during centrifugation. As a result, coverslips of size 2 were then used, which had better strength. To ensure that cells did not stick to the walls of the PDMS devices, Bovine serum albumin (50 mg/mL, sterile filtered) was added in the devices with a syringe pump and the chips were incubated at 37°C for one hour. Magnesium sulfate (MgSO₄.7H₂O, 10mM final concentration, sterile filtered) was added to LB media while growing the cells to prevent cells from forming clumps/biofilm. A mix of LB broth and BSA (5:1 ratio) with 10 mM magnesium sulphate was then used to wash cells from the mother machines and to observe their growth (hereafter referred to as wash fluid).

2.5 Particle image velocimetry in interaction zone

Red fluorescent latex beads (carboxylate modified polystyrene, Sigma Aldrich) mixed in with wash fluid were added to the devices under different flow rates to estimate the speed of beads in the interaction zones. The PDMS device was primed with BSA as described above and incubated at 37°C for an hour. Following that, wash fluid mixed with the fluorescent beads was added to the device using syringe pump at different flow rates and it was visualized in real time using confocal microscope. The speed was calculated using ImageJ software for analysis by

measuring the length of the fluorescent streak created by movement of bead with the flow in the interaction zone and dividing that distance by the exposure time for taking the image (speed= distance/ time).

2.6 Time Series Experiment with Antibiotics

The time series experiment was conducted for devices with and without addition of antibiotics. In case of no antibiotics, after the wash, the flow of media was reduced to 1 $\mu\text{L/hr}$ and growth of cells in the mother machines and their pushing out into the interaction zone was observed for 4 hours. Images under bright field and RFP lights were taken every 30 minutes. In the experiment with antibiotics, the antibiotic Ampicillin (Ward's Science, ON) in sublethal concentration (8 $\mu\text{g/mL}$) (Baltekin et al. 2017) was added to the media and flow was initially started at 1 $\mu\text{L/min}$ to fill the devices and then reduced to 1 $\mu\text{L/hr}$ for the duration of time series experiment.

2.7 Time series experiment with less fit mutant and wild type

Keio mutant 69A4 (least fit mutant, Table 1) and fluorescent wild type *E. coli* were grown in LB broth with added magnesium sulfate overnight. Their OD at 600 nm was measured on a NanoDrop and equal amounts of OD was taken to concentrate the cells by centrifugation at 5000 rpm for 5 minutes. The pellets were resuspended in supernatant to reduce the volume to 1/10th of the original volume, similar to previous experiments. Both types of cells were thus mixed in equal amounts to create a combined culture. The rest of the experimental protocol and setup was same as described above.

3.0 Results and Discussion

3.1 Mutant Screening Platform Design and Fabrication

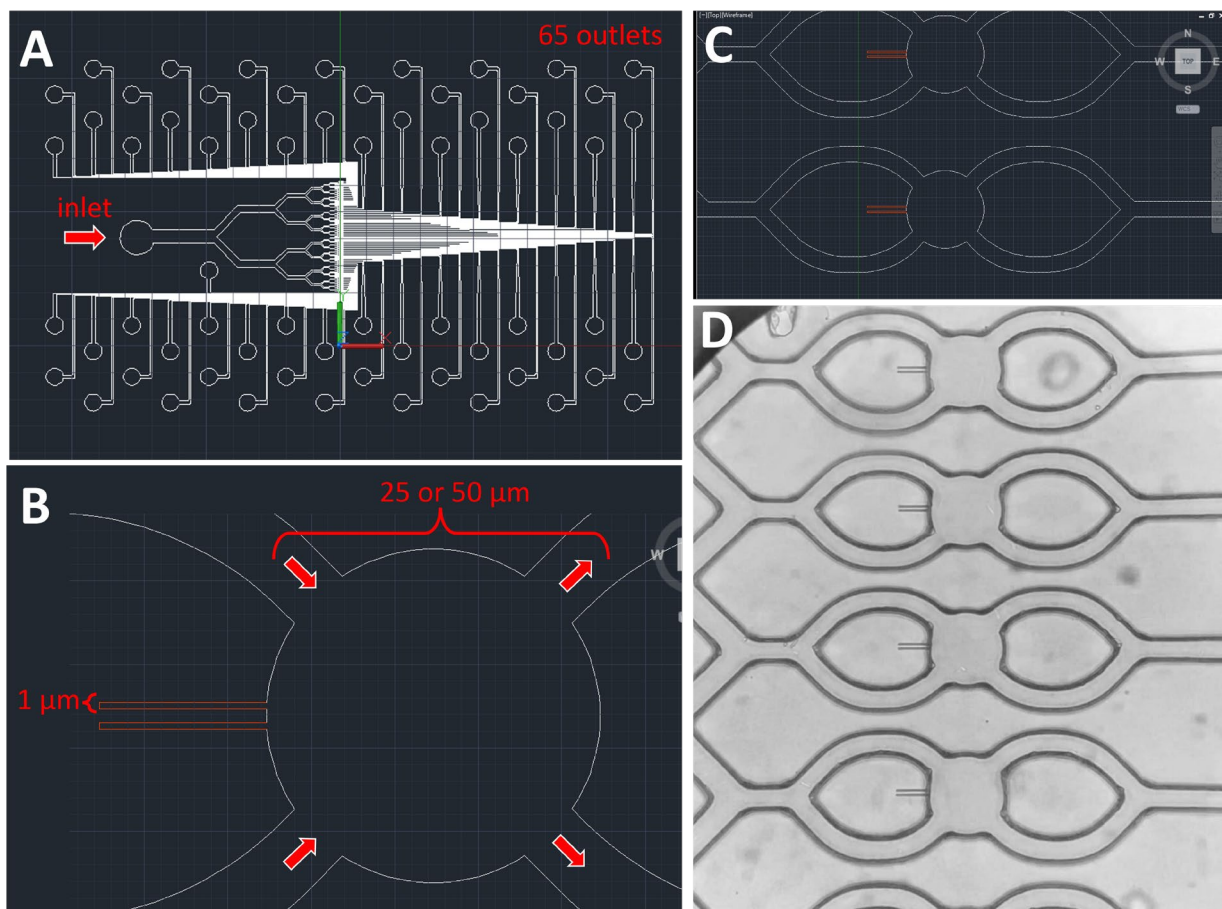


Figure 2: A) The microfluidic mutant screening platform was designed to have one inlet and 65 interaction zones, each with their own outlets for high-throughput experimentation. B) Two mother machines (1 μ m wide, 25 μ m long) seed each interaction zone (25 or 50 μ m wide). C) the AutoCAD design includes two layers: 1.4 μ m deep mother machines (red), 20 μ m deep other channels (white). D) A brightfield image of the PDMS mold shows the replication accuracy of the design.

3.2 Bulk Competition Experiments

In order to benchmark the efficacy of the microfluidic mutant screening approach, we first performed bulk competition experiments between cell lines using conventional bulk competition experiments in a well plate format.

There were no differences between fluorescent (F) parent sample and the fluorescent (F)-non-fluorescent (NF) parent mix sample, confirming that introducing genes for the fluorescent protein did not affect the fitness of *E. coli* (Table 1). No differences were observed between

fluorescent parent-equal fit mutant mix samples and fluorescent- non-fluorescent parent mix sample, which was expected. The percentage of fluorescent cells in mix of fluorescent parent-less fit mutant samples was significantly higher than F+NF parent. The percentage of fluorescent cells in fluorescent parent-more fit mutant sample was significantly lower than F+NF parent.

Table 2.

Percentage of fluorescent cells from mixed cultures as calculated from Novocyte flow cytometer

Sample	% Fluorescent cells
Fluorescent parent + non-fluorescent parent	60.1 +/- 5.6 %
Fluorescent parent + equal fit mutant	66.6 +/- 9.2 %
Fluorescent parent + less fit mutant	91.6 +/- 1.9 %
Fluorescent parent + more fit mutant	26.3 +/- 4.8 %

3.3 Particle image velocimetry and flow simulations in interaction zones

In order to maintain sub-populations of a constant size in each interaction zone, there must be an equal flow rate through each interaction zone. Similarly, the design must allow for slow enough velocities within each interaction zone turbidostat such that the flow through the interaction zone results in the same number of cells being washed out per doubling time as were created.

To inform the design of the 65 parallel interaction zones and their input and output channels, we simulated the fluid dynamics within the channels in COMSOL before fabricating them. The channel lengths and widths were optimized so that the pressure across each interaction zone was equal assuming an inlet flow rate of 1 $\mu\text{L/h}$ which is the minimum flow rate that can be attained with a conventional syringe pump. Under these input parameters, the flow velocities through each interaction zone were approximately 0.01 $\mu\text{m/s}$, well below the swimming speeds of an average *E. coli* cell which allows the progeny cells to self-mix within the interaction zone (Figure 3).

To determine the actual velocities within the interaction zones, we used particle image velocimetry, a method that involves flowing fluorescent beads through the channels and imaging the distance they travel over a given exposure time. Although some of the beads stuck to the walls on the device, most of them could be observed moving by producing a fluorescent streak under flow. The range of speeds in the top part of interaction ranged from 33-43 $\mu\text{m/s}$, while it ranged from 40-45 $\mu\text{m/s}$ under flow rates of 1 $\mu\text{m/min}$ and 0.5 $\mu\text{m/min}$. In the bottom part of interaction zone, that is, when the beads were flowing towards the outlets, the speed increased to 60-81 $\mu\text{m/s}$.

In some interaction zones, opposite flow of fluid (towards the inlet) was observed after stopping the flow from syringe pump. This could probably be due to complex pressure

gradient dynamics created by insertion of tube in the inlet. The particle image velocimetry confirmed that velocities within the interaction zones can be finely tuned by tuning the input flow rate to match the doubling times of *E. coli* cell populations.

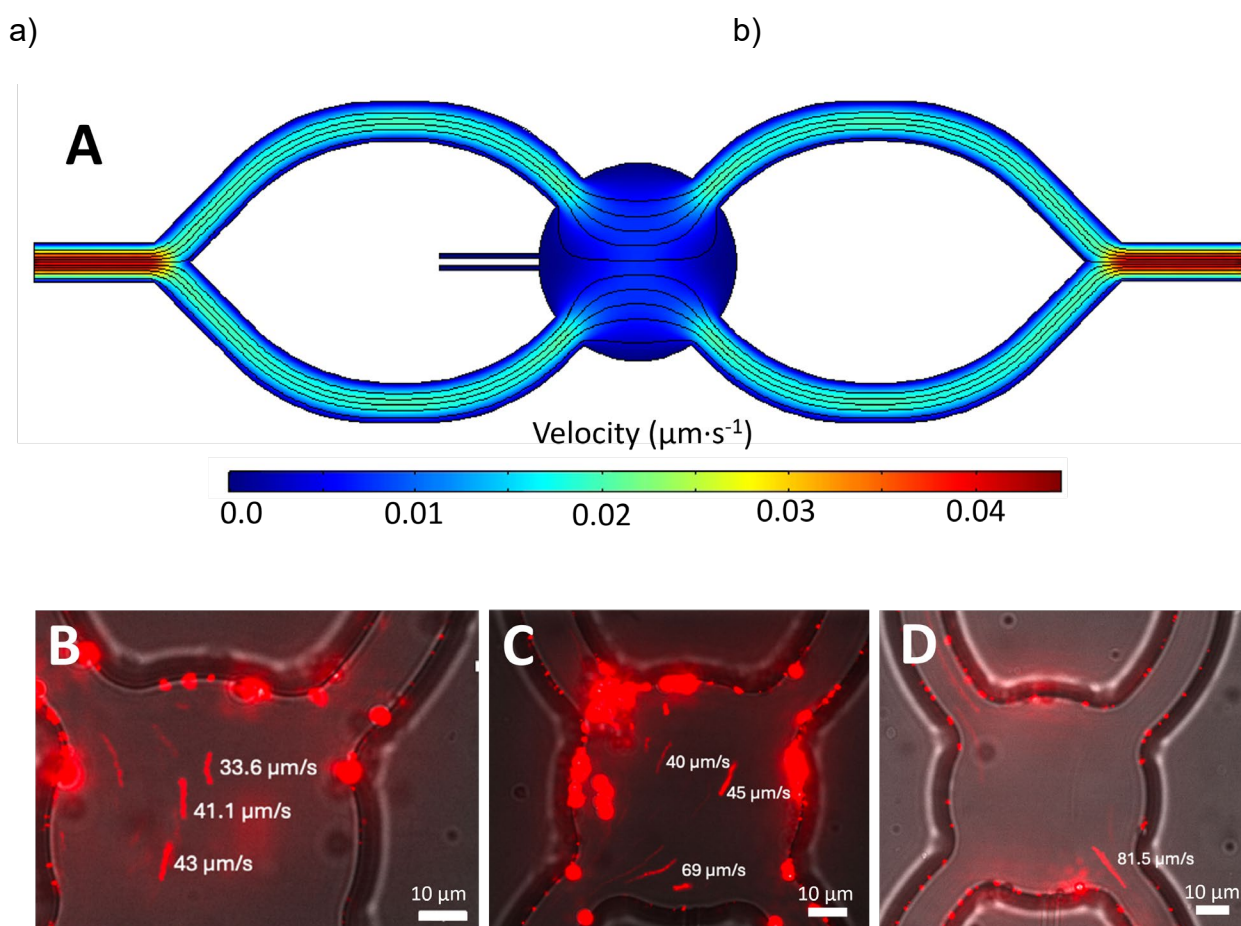


Figure 3 : Particle image velocimetry of interaction zones. A) Laminar flow simulations (COMSOL) through the interaction zones show theoretical velocities down to $0.01 \mu\text{m/s}$ in the when flow to the design inlet was set to $1 \mu\text{L/hr}$. Speeds of fluorescent beads under flow of a) $1 \mu\text{L/min}$, b) $0.5 \mu\text{L/min}$ and c) $10 \mu\text{L/hr}$ were calculated using particle image velocimetry.

3.4 Mother machine seeding and wash out

Next we optimized the loading of *E. coli* cells to the microfluidic mutant screening platform. Initial rounds of adding *E. coli* fluorescent wild type cell culture without concentrating it by centrifugation did not give any success in seeding mother machines with cells, even after

centrifugation. After concentrating the cells by centrifugation, centrifuging and incubating overnight, at least 7-8 mother machines out of 65 were seeded. The number of channels seeded with cells was random in each experiment. This was perhaps due to the unique design of the device which had individual interaction zones for mother machines.

Overnight incubation with a flow of 1 $\mu\text{l/hr}$ (LB+ BSA+ MgSO_4) helped greatly with the seeding of mother machines and reducing clogging in narrow channels. When the flow was increased to 1-2 $\mu\text{l/min}$ for washout after overnight incubation, it was observed that some of the interaction zones were washed out of all cells within 2-3 minutes of starting the flow, while some remained filled, probably due to clogging of main channels. When back flow from outlets was started, in most cases the wash fluid (LB+BSA+ MgSO_4) came out of nearby outlets or the inlet, but in some cases, it backed up from the same outlet. This could again be due to clogging in narrow channels. It was observed that while BSA did help with reducing sticking of cells on walls and clogging, some clogging still persisted. Back wash from outlets helped in clearing some clogs.

3.5 Cell Replication in Mother Machines

Once the mother machines were seeded with cells, their replication was observed while flow through the platform was started at 1 $\mu\text{l/hr}$. Images taken 30 minutes apart showed *E.coli* cell dividing into two daughter cells in mother machines.

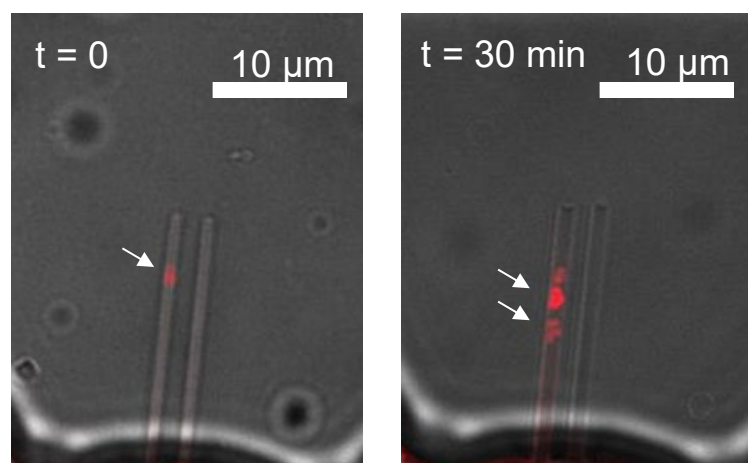


Figure 4: Time series images of *E.coli* mother cells in mother machines dividing into two daughter cells. Images were taken every 30 minutes on confocal microscope under 63X in bright field and RFP light

3.6 Continued replication and inoculation of interaction zones

After wash out and incubation, when at least 7-8 mother machines were seeded with *E.coli* cells, a time series experiment was started to image *E.coli* replication and growth. It was observed that incubation after wash out greatly helped in replication of cells and filling of mother machines with *E.coli*. Another wash out after incubation was necessary to wash out the recently divided daughter cells from interaction zones. Continuous flow of 1 $\mu\text{l/hr}$ helped with *E.coli* growth in mother machines. When a mother machine was filled with cells, the daughter cells were pushed out into the mother machines. In the interaction zone, in many cases cells were washed away with the flow.

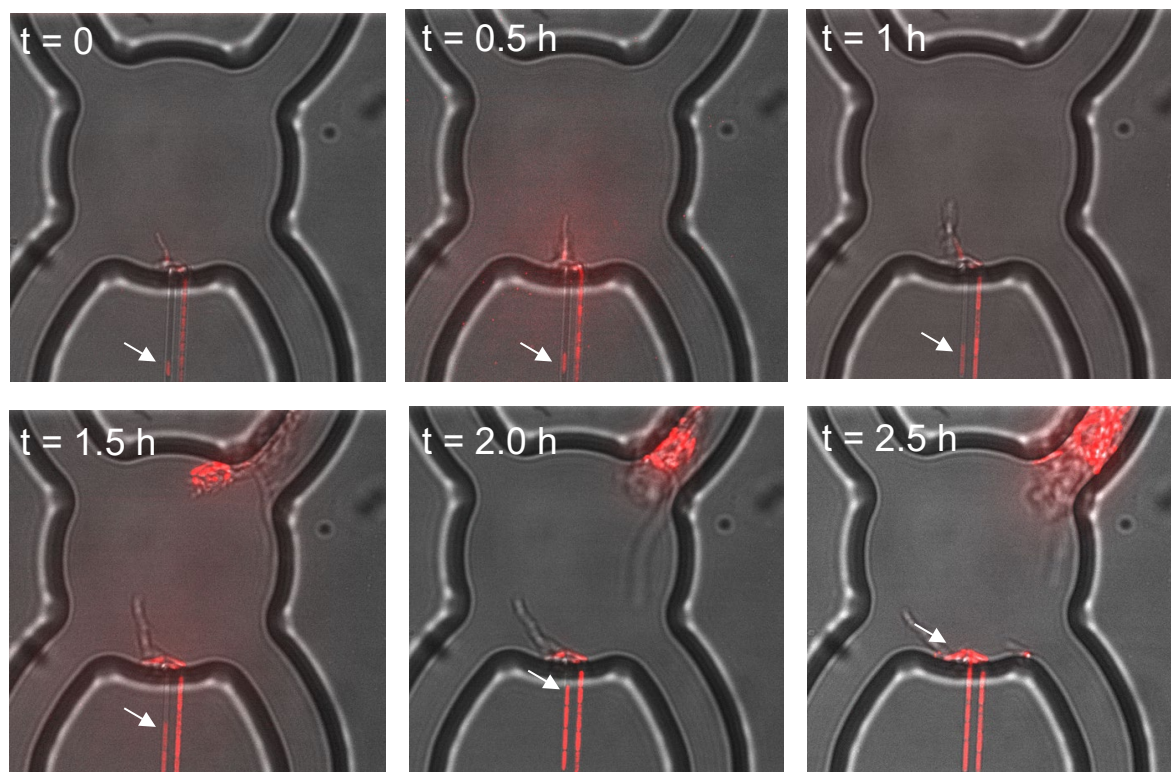


Figure 5 Time series images showing growth of cells in mother machines and pushing daughter cells in the interaction zone

3.7 Growth in presence on antibiotic Ampicillin

The microfluidic mutant screening platform has the potential to act as an antibiotic susceptibility screen for microbes by measuring their grown rates at the single cell level. It was observed that sublethal concentration of Ampicillin did not stop the growth of *E.coli* wildtype cells seeded in mother machines. Cell division in mother machines was observed in presence of ampicillin with roughly the same doubling time (30 min) as without the antibiotic. It is possible that the concentration of ampicillin needs to be increased to induce a measurable reduction in cell reproduction rates or that multiple mother machines need to be monitored to collect enough data to see an average reduction in population growth.

3.8 Competition between wildtype and mutant strains

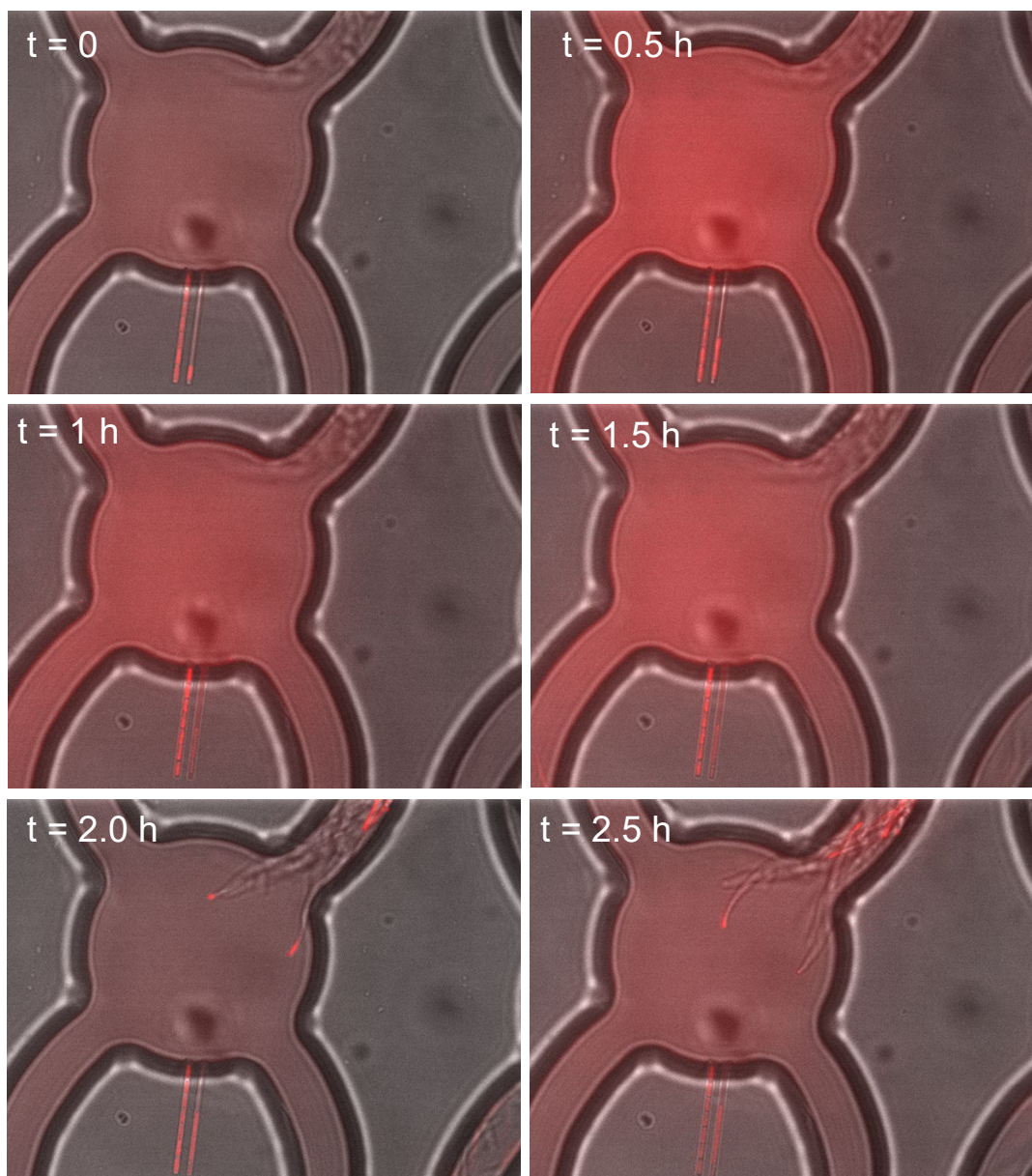


Figure 6. Time series images taken every 30 minutes of growth of *E.coli* cells in mother machine in presence of Ampicillin

When less fit mutant and fluorescent wildtype *E.coli* were added to the device, the majority of mother machines that were seeded contained either only mutant cells (non-fluorescent) or only fluorescent wildtype cells. This was expected because the design relies on random chance to seed the mother machines with a cell type. However, we observed 2-3 cases where one mother machine was seeded with a fluorescent cell and the second was seeded with mutant cells in the same interaction zone. Division of cells in mother machines and pushed out into interaction zones was clearly observed under flow of $1\mu\text{l/hr}$.

When a single mother machine was seeded with both fluorescent wildtype cell and a non-fluorescent mutant cell, the cell that is at the dead end of the mother machine becomes the

mother cell and the other cells are eventually pushed into the interaction zone through replication (figure 7, time 0 to time 1h).

In this proof-of-concept experiment, the fluorescent wildtype strain “won” the competition against the less fit, nonfluorescent mutant after 1.5 hours. At the end of the experiment (2 hours), the interaction zone was washed out by increasing flow rate to the mutant screening platform so that no cells remained in the interaction zone. After the wash-out, mother cells remained in the mother machines and these could be used to repeat the experiment again.

This proof-of-concept experiment demonstrates the utility of this mutant screening approach. However, many more experiments would need to be run with the same WT vs. mutant competition in order to generate a “probability of fixation” value based on the outcome of the competition. If these experiments are done in the future, then they can be compared to the conventional bulk competition experiments to confirm whether the microfluidic screen reduces error in cell fitness predictions as expected.

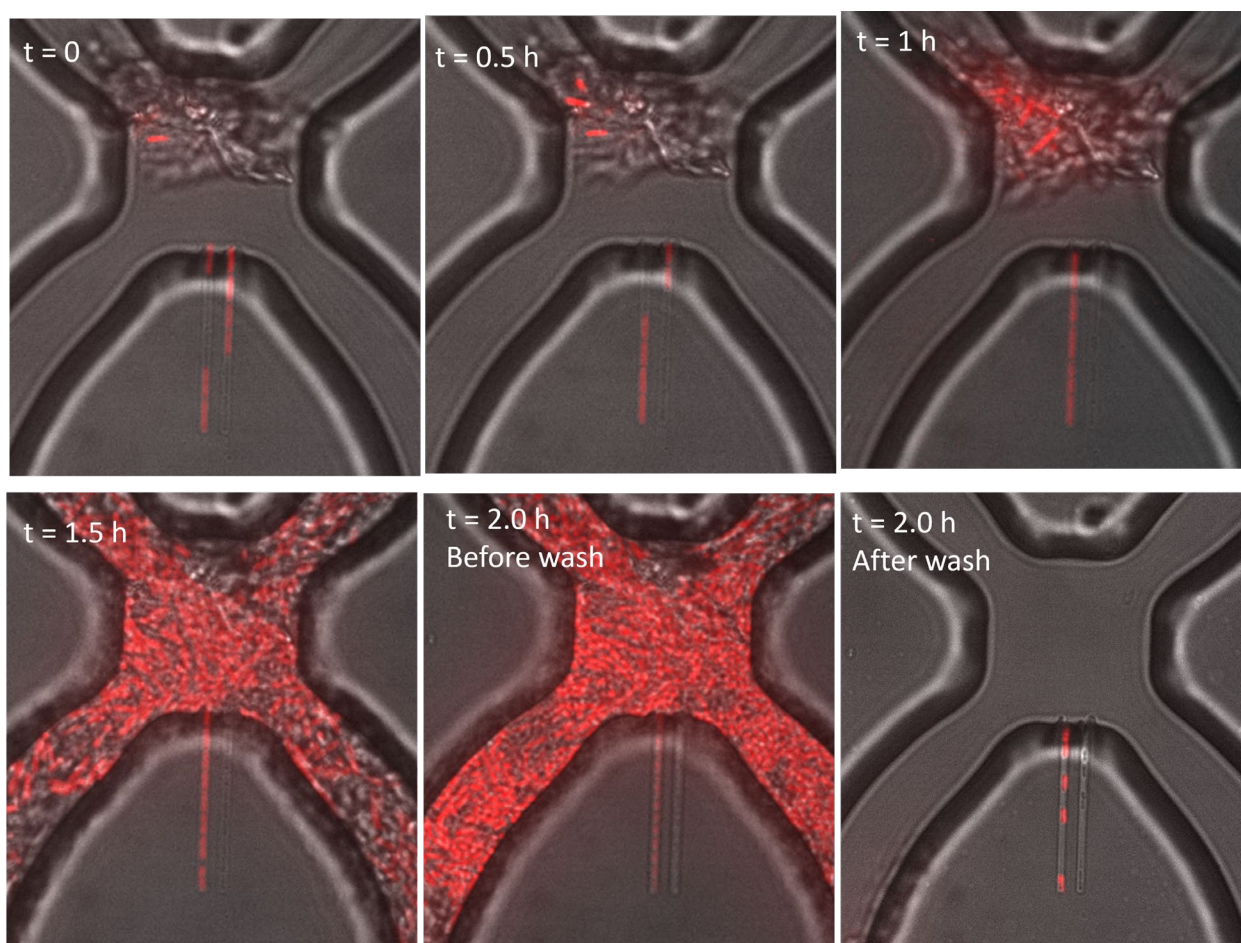


Figure 7. Time series images of growth of less fit mutant and parent wildtype E.coli (red fluorescent) cells in mother machines

4.0 References

- (1) Dusny, C.; Schmid, A. Microfluidic Single-Cell Analysis Links Boundary Environments and Individual Microbial Phenotypes. *Environmental Microbiology* 2015, 17 (6), 1839–1856. <https://doi.org/10.1111/1462-2920.12667>.
- (2) Mehling, M.; Tay, S. Microfluidic Cell Culture. *Current Opinion in Biotechnology* 2014, 25, 95–102. <https://doi.org/10.1016/j.copbio.2013.10.005>.
- (3) Wang, P.; Robert, L.; Pelletier, J.; Dang, W. L.; Taddei, F.; Wright, A.; Jun, S. Robust Growth of Escherichia Coli. *Current Biology* 2010, 20 (12), 1099–1103. <https://doi.org/10.1016/j.cub.2010.04.045>.
- (4) Postek, W.; Garstecki, P. Droplet Microfluidics for High-Throughput Analysis of Antibiotic Susceptibility in Bacterial Cells and Populations. *Acc. Chem. Res.* 2022, 55 (5), 605–615. <https://doi.org/10.1021/acs.accounts.1c00729>.
- (5) Arnoldini, M.; Vizcarra, I. A.; Peña-Miller, R.; Stocker, N.; Diard, M.; Vogel, V.; Beardmore, R. E.; Hardt, W.-D.; Ackermann, M. Bistable Expression of Virulence Genes in Salmonella Leads to the Formation of an Antibiotic-Tolerant Subpopulation. *PLOS Biology* 2014, 12 (8), e1001928. <https://doi.org/10.1371/journal.pbio.1001928>.
- (6) Scheler, O.; Postek, W.; Garstecki, P. Recent Developments of Microfluidics as a Tool for Biotechnology and Microbiology. *Current Opinion in Biotechnology* 2019, 55, 60–67. <https://doi.org/10.1016/j.copbio.2018.08.004>.
- (7) Long, Z.; Nugent, E.; Javer, A.; Cicuta, P.; Sclavi, B.; Cosentino Lagomarsino, M.; Dorfman, K. D. Microfluidic Chemostat for Measuring Single Cell Dynamics in Bacteria. *Lab Chip* 2013, 13 (5), 947. <https://doi.org/10.1039/c2lc41196b>.
- (8) Control, C. for D.; Prevention. Antibiotic Resistance Threats in the United States, 2019; US Department of Health and Human Services, Centres for Disease Control and ..., 2019.
- (9) Li, H.; Hsieh, K.; Wong, P. K.; Mach, K. E.; Liao, J. C.; Wang, T.-H. Single-Cell Pathogen Diagnostics for Combating Antibiotic Resistance. *Nat Rev Methods Primers* 2023, 3 (1), 1–23. <https://doi.org/10.1038/s43586-022-00190-y>.
- (10) Bergmiller, T.; Andersson, A. M. C.; Tomasek, K.; Balleza, E.; Kiviet, D. J.; Hauschild, R.; Tkačik, G.; Guet, C. C. Biased Partitioning of the Multidrug Efflux Pump AcrAB-TolC Underlies Long-Lived Phenotypic Heterogeneity. *Science* 2017, 356 (6335), 311–315. <https://doi.org/10.1126/science.aaf4762>.
- (11) Baba, T.; Ara, T.; Hasegawa, M.; Takai, Y.; Okumura, Y.; Baba, M.; Datsenko, K. A.; Tomita, M.; Wanner, B. L.; Mori, H. Construction of Escherichia Coli K-12 In-frame, Single-gene Knockout Mutants: The Keio Collection. *Molecular Systems Biology* 2006, 2 (1), 2006.0008. <https://doi.org/10.1038/msb4100050>.

- (12) Nichols, R. J.; Sen, S.; Choo, Y. J.; Beltrao, P.; Zietek, M.; Chaba, R.; Lee, S.; Kazmierczak, K. M.; Lee, K. J.; Wong, A.; Shales, M.; Lovett, S.; Winkler, M. E.; Krogan, N. J.; Typas, A.; Gross, C. A. Phenotypic Landscape of a Bacterial Cell. *Cell* 2011, 144 (1), 143–156. <https://doi.org/10.1016/j.cell.2010.11.052>.
- (13) Baltekin, Ö.; Boucharin, A.; Tano, E.; Andersson, D. I.; Elf, J. Antibiotic Susceptibility Testing in Less than 30 Min Using Direct Single-Cell Imaging. *Proc. Natl. Acad. Sci. U.S.A.* 2017, 114 (34), 9170–9175. <https://doi.org/10.1073/pnas.1708558114>.

Pacific Northwest National Laboratory

902 Battelle Boulevard
P.O. Box 999
Richland, WA 99354

1-888-375-PNNL (7665)

www.pnnl.gov